ANALYTICAL SCIENCES FEBRUARY 2010, VOL. 26

Reviews

Appearance Potential Spectroscopy (APS): Old Method, but Applicable to Study of Nano-structures

Y. FUKUDA

Research Institute of Electronics, Shizuoka University, 3-5-1 Johoku, Naka, Hamamatsu 432-8011, Japan

An old surface analytical method, appearance potential spectroscopy (APS), which can probe empty electronic states, is briefly reviewed, since it has an ability to be applied to studying nanostructures. Although the theoretical calculation of the APS spectra including a two-electron process is not much simpler than that of x-ray absorption spectroscopy (XAS) spectra with a one-electron process, measurements of the APS spectra are simpler than those of the XAS ones. A careful interpretation of the spectra would lead to a characteristic and simple surface chemical analysis.

(Received November 16, 2009; Accepted December 21, 2009; Published February 10, 2010)

1 Introduction

Surface analysis stands at a very important position for studying solid surfaces. X-ray photoelectron spectroscopy (XPS) and Auger electron spectroscopy (AES) have very often been used for the characterization of solid surfaces. XPS analyzes photoelectrons emitted by the ionization of core-levels with x-ray. The ionization energy is characteristic for atoms, and depends upon the chemical states of the atoms. Therefore, XPS is usually applied to elemental and chemical analyses of surface atoms. However, since XPS uses x-ray as an incident beam, it is generally difficult to focus the beam although recently various methods are used.

AES analyzes Auger electrons emitted by the ionization of core-levels with the primary electron, which can be focused to a μm - nm size. Both the methods measure filled electronic states using an electron energy analyzer, resulting in a high cost for making the apparatuses. On the other hand, appearance potential spectroscopy (APS) probes empty electronic states without any electron or optical energy analyzers, which are described in Chap. 3.

Soft x-ray is emitted by the excitation of core electrons with electron bombardment of solids. The electronic structures of metals had been studied by analyzing the emitted soft x-ray at constant electron energy with a grating method or by measuring a threshold energy appearing of the soft x-ray as a function of the applied electron energy. The latter method had a disadvantage that a large background intensity was superimposed on weak threshold signals.

In 1954 electric differentiation devices were applied to the latter method, resulting in obtaining clear Cu $3p_{3/2}$ and $3p_{1/2}$ spectra.[1] Two types of spectra, corresponding to a clean Cu surface and a "disturbed state", were found. In 1970, Park *et al*. developed and reported on "a soft x-ray appearance potential spectrometer" for the analysis of solid surfaces.[2] After this report many experimental and theoretical studies on APS have been reported and review articles were also presented.[3-9] However, the studies on APS decreased in 2000s in spite of the simplicity of the method. This would be due to the fact that x-ray absorption spectroscopy (XAS), which can also probe empty electronic states as well as APS, became popular because synchrotron radiation facilities can be easily used. The other reason would be that the excitation mechanism for XAS is simpler than that for APS, resulting in the easy theoretical calculation of XAS data measured on solid materials.

Since APS uses electrons as an incident (primary electron) beam, the electron beam can be focused to nano-meter size and spin-polarized. Therefore, APS could be applied to study empty states (chemical and magnetic states) of nanostructures although it is an old method.

In this review the followings are briefly described: the mechanism of APS, instruments, theoretical results, experimental results of metals, magnetic materials, compounds, chemisorptions and reactions, depositions, and fine structures.

2 Mechanism of APS[3]

A simplified APS mechanism could be described in four steps:

E-mail: royfuku@rie.shizuoka.ac.jp

(I) The primary electrons are irradiated on a solid sample. (II) The electrons are captured in empty levels and simultaneously core-electrons just ionized are excited to the empty levels (two electrons exist in the empty levels simultaneously, which is totally different from the other spectroscopy), which leaves core holes. (III) The excited states (II) are relaxed, resulting in the emission of soft-x-ray and Auger electrons through filling the core holes. (IV) The emitted total soft-x-ray or Auger electrons are collected as a function of the primary electron energy. Although the core holes interact with electrons in step (II), which leads to changes in energy and electronic structures, they are neglected here because of simplification. However, they are discussed in Chap. 4. In experiments primary electrons with increasing energy are irradiated on the solid surfaces and the total intensity of soft-x-ray (soft-x-ray appearance potential spectroscopy: SXAPS) or Auger electron (Auger electron appearance potential spectroscopy: AEAPS) is measured as a function of the primary electron energy, resulting in obtaining the APS spectrum.

The APS mechanism could be more quantitatively explained as follows. Figure 1 shows a schematic illustration of the energy diagram for SXAPS. E_{FC}, E_{FS}, and $N_V(E)$ represent the Fermi level of a thermal electron gun and sample (metal here), and density of filled states for core-levels, respectively. When a voltage V is applied on the electron gun using a thermal emitter, the electron energy on the sample is $e_V + \Phi_c$ (work function of the thermal emitter at temperature T) + k_T (thermal broadening of the electron energy at T). The electrons impinged into a solid sample are captured in an empty level, ε_1 and on the other hand, core electrons are simultaneously excited into an empty state, ε_2. Soft x-ray ($h\nu$) detected in SXAPS is emitted in the relaxation process. This total soft x-ray intensity is measured as a function of the primary electron energy.

Auger electrons are also emitted in the relaxation process and then the sample currents are abruptly decreased by the Auger electron emission. Changes in the sample currents are measured for AEAPS as a function of the applied voltage. When quasi-elastic scattered electrons are measured as a function of the applied voltage, the currents would be abruptly decreased at the Auger electron emission threshold. This is disappearance potential spectroscopy (DAPS).

Taking account of the energy conservation and binding energy (threshold energy), E_B, for the core-level,

$$e_V + \Phi_c + k_T = E_B + \varepsilon_1 + \varepsilon_2 \quad (1)$$

is obtained. Equation (1) becomes $e_V + \Phi_c + k_T = E_B$ at the ionization threshold of the core electron since both the primary and excited core electrons are just above the Fermi level ($\varepsilon_1 = \varepsilon_2 = 0$). The threshold energy, E_B, can be obtained since Φ_c (tungsten) and k_T are 4.52 (at 2800 K)[10] and 0.24 eV, respectively.

The transition rate, $T(E)$, of the primary and core electrons to empty states at E is expressed as

$$T(E) \propto \int_0^E \int_0^{E'} N_c(E'')N_c(E'-E'')\mathrm{d}E'' \times N_I(E+E_B-E')\mathrm{d}E', \quad (2)$$

where $N_c(E)$ and $N_I(E)$ correspond to density of empty states for one-electron and that of filled states for the excited core-level, respectively. Since the density of states of the core-level, $N_I(E + E_B - E')$, is generally assumed to be a delta function (= 1), the transition rate is expressed as

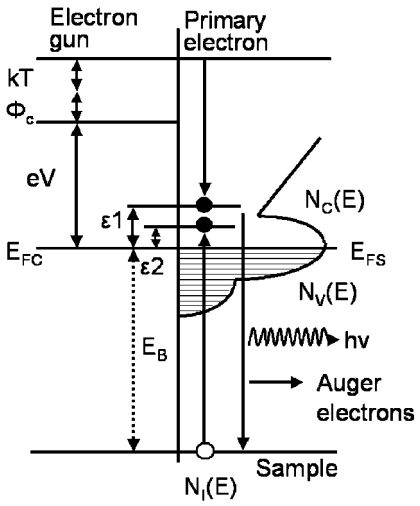

Fig. 1 Schematic illustration of the simplified APS process. Primary electrons with $e_V + \Phi_c + k_T$ are irradiated on a sample surface, resulting in capture of the primary electron into the empty level ε_1 and simultaneously in excitation of a core electron (binding energy E_B and density of the core-level, $N_I(E)$) to the empty level ε_2, which leaves a core hole (an open circle). Soft x-ray ($h\nu$) and Auger electrons are emitted in the relaxation process by filling the core hole, where k_T is thermal broadening of the primary electron; Φ_c, the work function of the emitter; E_{FC}, Fermi level of the emitter; E_{FS}, Fermi level of the sample; $N_V(E)$, density of filled states of the sample; and $N_C(E)$, density of empty states of the sample.

$$T(E) \propto \int_0^E N_c(E')N_c(E-E')\mathrm{d}E'. \quad (3)$$

This means that the rate (spectral shape) is proportional to self-convolution of the density of empty states for the one-electron system because there exist two electrons (both the primary and excited core electrons) in the empty states in the final states. This is schematically shown for 3d transition metals in Fig. 2, where the shaded and open (above the Fermi level E_F) areas in $N(E)$ represent densities of filled and empty states for the one-electron system, respectively. The density of empty states for a two-electron system, $N_{2C}(E)$, and the derivative $\mathrm{d}N_{2C}(E)/\mathrm{d}E$ are also shown in Fig. 2. Therefore, if the measured APS spectra are self-deconvoluted, the density of the empty states for atoms on the samples could be obtained although this is a simple consideration. Detailed theoretical calculations of the APS spectra were extensively carried out. The results are described in Chap. 4.

If a field emission gun is employed and sample currents are measured as a function of the applied voltage, the absolute work function of the samples could be easily obtained with high-resolution since $\Phi_c = 0$ and $k_T = 0.026$ eV at 300 K (see Fig. 1). The APS threshold energy could also be measured without any correction of the filament work function. This example is described in Chap. 5.

3 Instruments[11-32]

The first SXAPS apparatus[2] (Fig. 3) consisted of a nickel photocathode (quantum efficiency: 0.01 – 0.1) and a lock-in amplifier, the incident current density was about mmA/cm^2, and

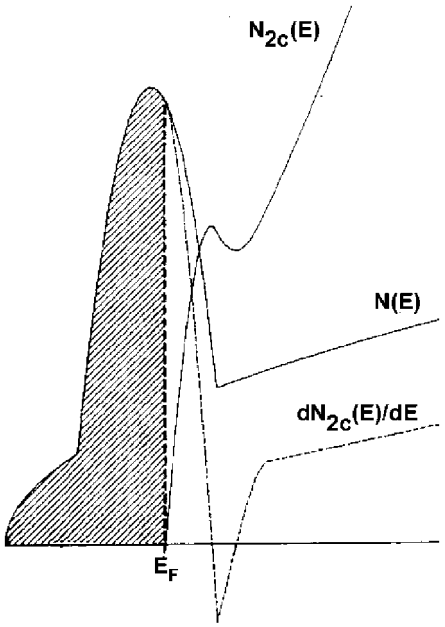

Fig. 2 Simple schematic representation of density of states in APS for 3d transition metals.[6] $N(E)$ denotes the one-electron density of states, where the shaded and open (above the Fermi level E_F) areas represent densities of the filled and empty electronic states, respectively. The two-electron density of the empty states $N_{2c}(E)$ is obtained by self-convolution of $N(E)$ above E_F. The APS derivative spectrum $dN_{2c}(E)/dE$ is shown.

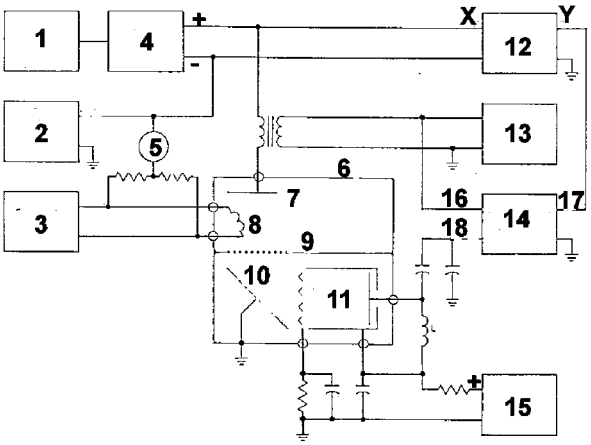

Fig. 3 Schematic illustration of the first SXAPS apparatus,[2] where 1 is a rump generator; 2, bias supply (+50 V); 3, filament supply; 4, programmable power supply (0 – 2 kV); 5, ammeter; 6, vacuum chamber; 7, sample; 8, filament; 9, shield; 10, photo-cathode; 11, electron multiplier; 12, x-y recorder; 13, oscillator (2.16 kHz); 14, phase-lock amplifier; 15, multiplier supply; 16, reference; 17, out; and 18, signal.

the pressure in the analytical chamber was as high as 10^{-7} Torr in operating.[2] Using a lock-in amplifier led to an explosive increase in following APS studies. A 6.3 μm thick aluminum foil filter was employed to cut off low energy soft x-ray for improvement of signal-to-noise ratio in APS and differentiation of the spectra directly measured without a lock-in amplifier succeeded using a computer.[11]

A sensitive detection system for SXAPS was constructed; it consisted of a 6-μm thick aluminum foil, a cesium iodide photocathode, a continuous-channel electron multiplier, and conventional pulse-counting electronics. This resulted in a reduction of the electron excitation current to a few μA/cm^2.[12] An interesting low noise SXAPS spectrometer was developed; it consisted of a liquid nitrogen-cooled silicon surface barrier diode to detect the emitted photon flux.[13] This achieved a $S/N \approx 20$. The primary electron currents could be reduced to less than 10 μA/cm^2 by using a channel plate detector.[14] A GaAsP spin-polarized electron source was first employed to study the magnetic properties of empty states.[15] A high-performance SXAPS spectrometer was designed and built, which consisted of an alkali halide (CsI) photon-to-electron converting layer evaporated onto an amorphous carbon foil.[16] This resulted in obtaining a signal-to-noise ratio of 150 at the diamond carbon peak.

AEAPS spectra were first obtained on disordered Ba and W(100) surfaces by differentiation of the secondary electron yield as a function of the primary electron energy.[17,18] In this measurement the potential of the electron gun was oscillated by an isolation transformer and swept by a programmable dc power supply. The ac current to the target was detected by a tuned tank circuit and phase-lock amplifier. It was pointed out that the experiment did not work with the single crystal W(100) surface because of exhibiting strong diffraction structures, which hide the threshold features.

DAPS spectra of a stainless-steel surface were first obtained using a conventional low-energy electron diffraction (LEED) apparatus.[19,20] This method detects a decrease in the elastically backscattered electron current at characteristic excitation thresholds of the surface atoms when the primary energy is scanned.

Since the APS methods detect the total x-ray emitted or the total electrons emitted or the decreased elastically scattered electrons as a function of the applied voltage on the samples, no optical (or electron) analyzers are required, resulting in building them easily.

4 Theoretical Results[33-48]

A simple theoretical consideration on APS is described in the previous chapter. In this chapter more sophisticated theoretical calculations on the APS process and various phenomena in APS are briefly reviewed.

Threshold singularities in APS were discussed using a model Hamiltonian[33] and the anomalous edge behavior in simple metals was investigated.[39] The effect of plasmon production on the APS spectra of a simple metal (Al) was calculated within the framework of many-body perturbation theory.[38] In the 2p spectrum, the plasmon contributes very weak at the threshold energy for plasmon production. In the 1s spectrum, there was a finite contribution.

Calculations of the matrix elements for electron-induced ionization of core electrons of atoms were carried out using both self-consistent atomic potential and model potentials.[41] Particular attention to the angular momentum distribution of the two final-state electrons was paid. It was found that for sufficiently bound states, the "approximate selection rule" holds until the incident electron energy exceeds the ionization threshold by at least 500 eV.

Theories of APS were presented for interacting electrons in a nondegenenate energy band described within the frameworks of the Hubbard[44] and generalized multiband models.[45] It was

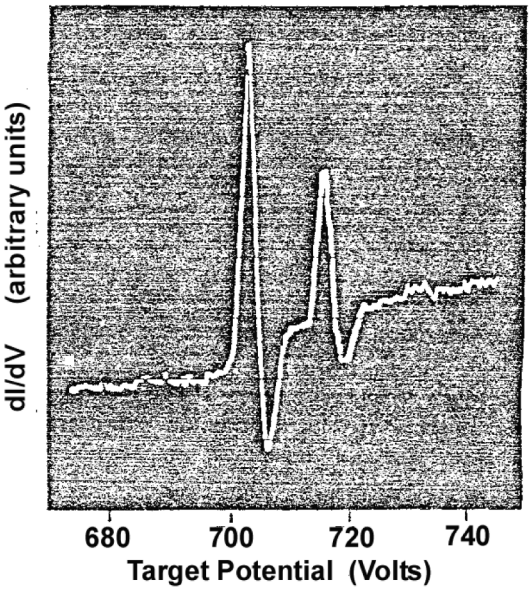

Fig. 4 First SXAPS Fe 2p spectrum of a clean Fe metal.[2]

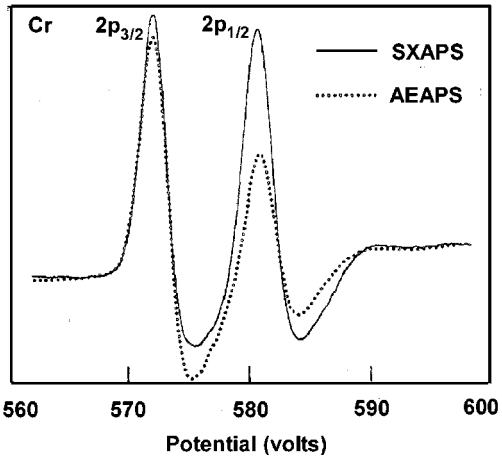

Fig. 5 SXAPS and AEAPS Cr 2p spectra of a clean Cr metal.[49]

pointed out that the simple self-deconvolution model for the two-particle spectral density turns out to be inappropriate for highly correlated electron systems. A theory that includes the effects of Coulomb interaction between the valence band electrons and the core electrons was presented.[46] It was concluded that the APS spectra are influenced by scattering at the core hole in the final state.

The three-particle spectral density in a generalized ladder approximation was calculated within the framework of the single-band Hubbard model. The APS spectra of heavy-fermion systems ($CeNi_5$ and $CePd_3$) were presented and analyzed within the framework of the Gunnarson-Schönhammer approach for the Anderson-impurity model.[47] It was indicated that this approach could describe two-particle response functions as reliably as those of one-particle spectra.

A theoretical description of spin-resolved APS was presented on the basis of a single-particle description of the underlying electronic structure.[48] Application of the formalism presented to bcc Fe and fcc Ni led to results in very satisfying agreement with corresponding experimental data.

5 Experimental Results on Metals[49-105]

Although many APS spectra were presented and listed in a period table in 1974,[9] new results after the review together with previous data are described in this and following chapters. The first APS spectra were measured on Ti, Fe, and C.[2] The SXAPS Fe 2p spectrum is shown in Fig. 4. It was pointed out that the $2p_{3/2}$ and $2p_{1/2}$ peaks are located at 704 and 716 eV, respectively, where the work function of the filament was not corrected. A lot of APS spectra of metals were presented after reporting this result.

Especially the 3d transition metals were widely studied using SXAPS and AEAPS.[49-66] The Cr $2p_{3/2}$ and $2p_{1/2}$ spectra of a chromium metal surface were measured using two methods, SXAPS and AEAPS (Fig. 5).[49] An interesting result was presented, that the $2p_{3/2}/2p_{1/2}$ intensity ratio in AEAPS is almost exactly 2, as compared to approximately 1 for SXAPS. It was pointed out that strong diffraction effects, which would be superimposed on an APS signal, were observed at an energy below about 200 eV.

The SXAPS $2p_{3/2}$, and $2p_{1/2}$ spectra of the 3d transition metals (Sc-Ni)[50] were presented and compared to the x-ray data.[67] Spin-orbit splittings determined by APS were in excellent agreement with the tabulated x-ray data. The binding energies (threshold energies) obtained by APS were found to be lower for the 3d transition metals than the tabulated values. The energies of Fe and Ni, and the 3d transition metals measured by conventional SXAPS[52] and AEAPS with a field emission gun,[55] respectively, were compared with the XPS data. The values obtained by APS were also found to be lower than those by XPS.

The Cu 2p spectrum was reported not to be found[50] but a weak one was detected.[3] The Cu $2p_{3/2}$ spectrum was self-deconvoluted and the result was compared with both experimental and theoretical results. The latter was in qualitative agreement with the APS result.[57]

The APS Fe $2p_{3/2}$ spectral shape of a Fe metal was found to agree well with the theoretical density of states above the Fermi level. It was demonstrated that considerable care has to be taken in discussing "binding energy" or "chemical shifts" as derived from different electron spectroscopic methods (APS and XPS).[53]

The density of empty electronic states in solid and liquid Ni was determined using AEAPS.[61] The observed increase in the density of states at the Fermi level by a factor of 1.4 in the liquid was in good agreement with resistivity data.

A comparison of measured and calculated APS $2p_{3/2}$ spectra for the 3d transition metals (Ti-Ni) was carried out.[64] The calculated spectra of Co and Ni using a simple one-electron model, in which both the excited core electron and the incident electron have final states near the Fermi level, were found to be in satisfactory agreement with the measured ones. It was pointed out that the measured spectra of Ti and V are in agreement with the calculated result including the core-hole effects and the effects are smaller for Cr and Fe, but still noticeable.

Contributions of electrons with different energies to AEAPS were investigated for Ti, Cr, Mn, and Ni using a spherical three-grid retarding field system.[66] The contribution was reported to show a big difference between the 2p and 2s spectra.

Rare-earth metals were also widely studied by APS.[68-81]

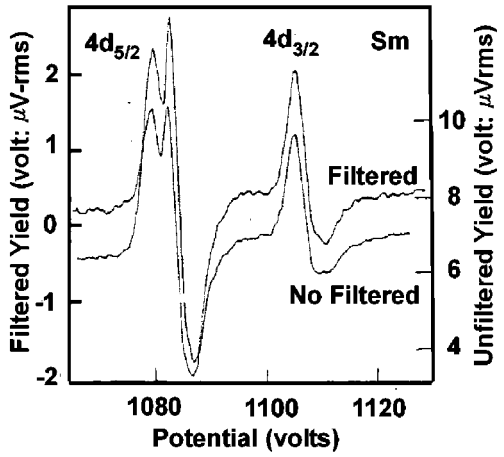

Fig. 6 The SXAPS Sm 4d spectra of a Sm metal with and without a 6.3-μm thick aluminum foil for prefiltering low-energy x-ray.[68]

Intensity singularities in SXAPS of Sm $4d_{5/2}$ and $3d_{5/2}$ levels were reported (Fig. 6).[68] It was indicated that excitation of the singularities depends upon both the energy of the incident electron and the angular momentum of the core state vacancy. The singularities were attributed to final state interactions between the inner vacancy and a two-electron bound state at the site of the core vacancy.

The SXAPS spectra of La ($3p_{1/2}$-4d levels), Gd ($3p_{3/2}$-4d levels), and Th (5d-4s levels) were measured and the binding energies were compared with those obtained by XPS and calculations.[69] The results were in reasonable agreement. Satellite peaks were observed associated with the 3d and 4d peaks of La and Gd, and the 5d peaks of Th. It was pointed out that the satellite peaks result from plasmon coupling between the collective modes of the conduction electrons and the core hole.

The strong spectral intensity of La, Ce, Pr, and Nd with only a few atomic percent in a NiCr alloy was observed, which was interpreted in terms of strong resonance interactions between the incident electrons and the atomic 4f states.[70] The $3d_{5/2}$ binding energies of La, Ce, Pr, and Nd were compared with those obtained by XPS and XAS.[72]

The SXAPS and AEAPS 3d spectra of La were also compared and the result concluded that bremsstrahlung does not dominate the spectral shape in APS (Fig. 7).[74] The structures in the 3d level of La were discussed in terms of the resonance x-ray emission. The 3d levels of La, Ce, Nd, Sm, Eu, Gd, Dy, and Er were measured and compared with the tabulated x-ray data.[75] No APS spectra of Pr, Tb, and Ho were found. Contrary to this result, significant intensities of the $3d_{5/2}$ and $3d_{3/2}$ spectra for Pr, Tb, and Ho were detected.[76] The intensity of APS peaks in rare earth metals was shown to depend on the total number of 4f electrons.

The $4d_{5/2}$ and $4d_{3/2}$ levels of the SXAPS and AEAPS spectra for La, Ce, Pr, Nd, and Sm were also measured. Both of the spectra exhibited multiplet structures below the expected 4d excitation threshold and a broad 10 – 20 eV wide peak above the threshold followed by small peaks of decreasing intensity.[78] Both of the spectra of the above-mentioned metals oxidized were also presented. The spectra for the oxidized surfaces did not show any major change in the spectral features except for a chemical shift of the threshold.[79]

A comparison of the 3d level spectrum of Y with that of La was made and showed that though the main peaks remained the same, additional fine structures appeared in the La spectrum. This was discussed in terms of empty localized 4f levels in La.[80]

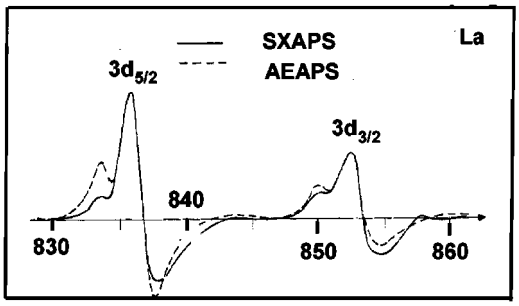

Fig. 7 AEAPS and SXAPS La 3d spectra of a La metal.[74]

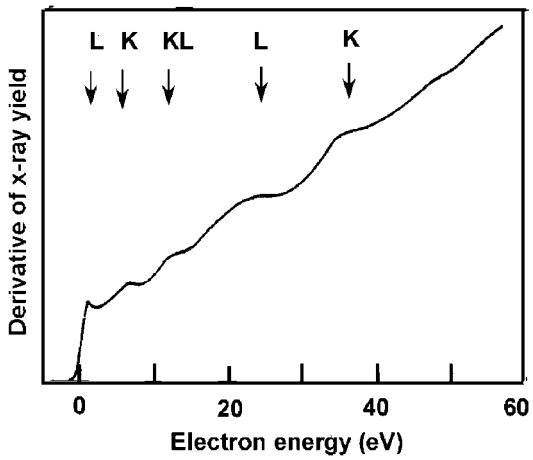

Fig. 8 SXAPS Al 2p spectrum of an Al metal. The arrows show the peak positions in the XAS spectrum.[84] K and L denote the peak positions of XAS K and L spectra of Al.

The APS spectra of the sp metals were reported.[82-91] The first measurement of the Al, Mg, and Be 2p levels was presented and a strong correlation between APS and XAS was found (Fig. 8).[84,88] Plasmon satellites were also observed for Mg and Be.

The SXAPS C 1s spectrum for graphite showed strong plasmon effects.[83,85,86] The SXAPS spectra of pyrolytic graphite were measured as a function of the angle of the incident electrons. Coupling with the fast incoming electrons was observed.[87]

The SXAPS Al 1s spectrum of Al was presented and a comparison of the spectrum with a calculation gave an evidence for the importance of the angular parts of the transition matrix elements.[90]

Diamond films were studied by SXAPS.[91] A comparison between the experimental spectra and spectra calculated using a theoretical empty density of states showed a reasonable agreement with respect to the energy position of the main spectral features. The result indicated that the spectra could clearly distinguish between sp^3-hybridized carbon (diamond) and sp^2-hybridized carbon (graphite).

Alloy surfaces were also widely investigated using APS.[92-105] A direct comparison of AES and APS was carried out for a 304 stainless steel, where S, C, O, Cr, Fe, and Ni were detected.[92] It was shown that the relative sensitivities of the two methods are strongly dependent upon the surface condition.

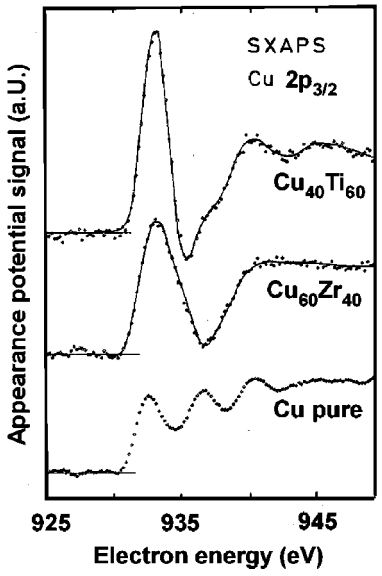

Fig. 9 SXAPS Cu $2p_{3/2}$ spectra of Cu, $Cu_{60}Zr_{40}$, and $Cu_{40}Ti_{60}$.[98]

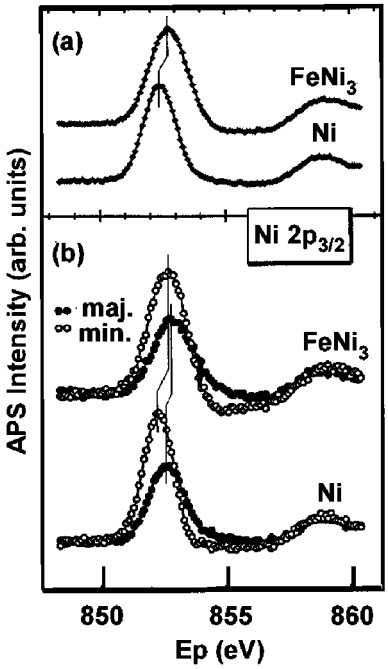

Fig. 10 Spin-integrated (a) and spin-resolved (b) SXAPS Ni $2p_{3/2}$ spectra of $FeNi_3$ and Ni.[112] The filled and open circles correspond to the majority and minority spins, respectively.

Fe/Ni alloys were studied by AES and APS and the "chemical shift" of Ni 2p was found to be decreased from 1.5 to 0.7 eV with decreasing Ni content.[94] The electronic structures of a NiFe alloy were investigated.[100,101] The result indicated a charge transfer from Fe to Ni in the alloy and suggested an enrichment of the Fe concentration and depletion of the Ni one on the surface. A study of the interaction of hydrogen with clean TiFe alloys using SXAPS was reported. It was found that the interaction at 800°C led to extensive Ti segregation.[96] APS measurements of Ti_xNi_{1-x} alloys suggested that charge transfer from Ti to Ni occurs.[97]

The local density of empty electronic states at the Cu sites in glassy $Cu_{60}Zr_{40}$ and $Cu_{40}Ti_{60}$ samples was derived from APS spectra (Fig. 9).[98] A narrow d-like density of states was found just above the Fermi level and the result was discussed in terms of d-band hybridization.

The APS spectra of the 3d levels of Dy and Er, and the 2p levels of Fe in pure metals and their intermetallics $DyFe_2$ and $ErFe_2$ were measured.[99] The widths of the Dy and Er peaks increased and that of the Fe decreased upon alloying, which was interpreted in terms of charge transfer from the rare earth to Fe.

The electronic structures of $Nd_2Fe_{15}B$ alloy were also studied by APS.[102] The changes in the binding energy (threshold energy) were interpreted in terms of the charge transfer from Fe to Nd. This was in agreement with theoretical calculations of the electronic structure of the alloy. An investigation of electronic structures of $Pr_2Fe_{14-x}Co_xB$ alloys was reported and the chemical shifts were discussed based on charge transfer among the constituents.[103] The spectral features were interpreted in terms of d-band narrowing as a result of interactions between the 3d bands of Fe and Co.

Two-particle spectra (APS spectra) of heavy fermion $CeNi_5$ and $CePd_3$ systems were measured and calculated.[104] The calculation described two-particle response functions as reliably as those of one-particle spectra. The SXAPS spectra of the 3d levels of Pr and Sm, and the 2p levels of Mn in $PrMn_2$ and $SmMn_2$ intermetallics were compared with the corresponding elemental spectra.[105] It was concluded that 3d-5d hybridization plays a significant role in determining the magnetic properties of these intermetallics.

6 Magnetic Materials[106-118]

Magnetic properties, especially empty electronic states have been studied using APS. The first APS study on this field was carried out for Ni and the threshold energy of the $2p_{3/2}$ level of Ni was found to remain constant with the annealing temperature even beyond the Curie point.[106] It was pointed out that this could not be reconciled with an interpretation based on a bandlike model.

The first direct observation of the spin-dependence of electron induced by core level excitations near the threshold using a polarized electron source (GaAsP) was reported for Fe.[107] The result could be understood by one-electron model calculations based on spin-split ground state densities of states above the Fermi level. The spin-dependent densities of empty electronic states in Fe and Ni were investigated by spin-resolved SXAPS (SR-SXAPS). Model calculations using the spin- and angular-momentum resolved densities of state with appropriate weighting were found to be in rather good agreement with the experimental results.[109]

The magnetic and structural properties of Fe/Cu(100) thin films were studied by spin-polarized APS and it was found that the spectral shape is sensitive to the crystal structure of the films.[110] This result demonstrated a direct correlation of the magnetism and structure. The temperature-dependent magnetic properties of the films were also investigated and the Curie temperature was found to be strongly decreased.[111] The results for Fe films on Cu(100) were interpreted to indicate the coexistence of a few ferromagnetically coupled Fe layers on top of noferromagnetic Fe layers.[114]

The electronic structure of the magnetic compound $FeNi_3$ was studied by spin-resolved SXAPS and the spectra were compared with results for pure elements.[112] The observed energetic shifts and spin-asymmetry changes (Fig. 10) were understood in terms of changes in the spin dependent local densities of states and in

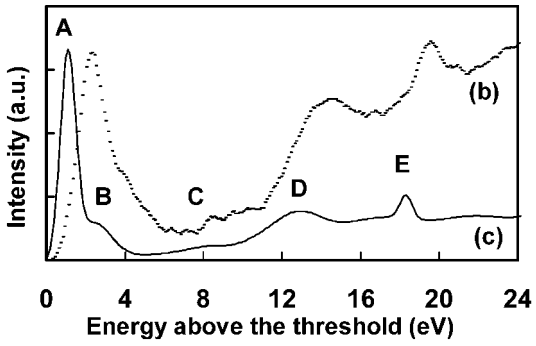

Fig. 11 Background subtracted Ni 2p APS spectrum of NiO(110) (b) and the self-deconvoluted spectrum (c).[143] Relative peak energies from A were found to be very close to those of XAS.

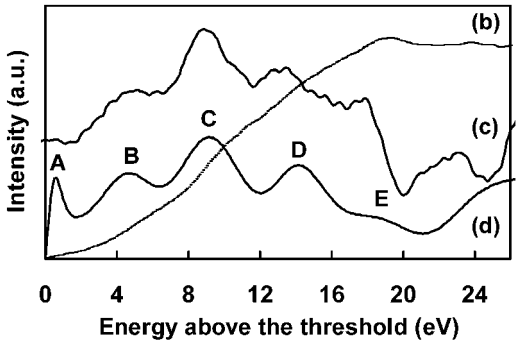

Fig. 12 Background subtracted O 1s APS spectrum of NiO(110) (b), derivative spectrum (c), and self-deconvoluted spectrum (d).[143] Relative peak energies from A were also found to be very close to those of XAS.

the core-level binding energies.

The magnetic properties of Fe films on W(100) were investigated and the spin asymmetry data showed a pronounced maximum at a film thickness of about 6 monolayers, which was attributed to the complex film morphology.[113] The magnetic properties of ultra-thin Cr/Fe layers on W(100) studied by SR-SXAPS were reported.[115] It was found that the magnetic moment of Fe at the Cr/Fe interface is reduced and the surface magnetic moment of an uncovered Fe film is enhanced.

The spin-dependent electronic structure at the ferromagnetic half-Heusler alloy NiMnSb(100) surface was studied by SR-SXAPS and the result was theoretically analyzed.[117,118] The spin asymmetry in the experimental results was found to be significantly reduced compared with calculations based on the bulk electronic structure.

7 Compounds[119-143]

Many APS studies on hydride, boride, nitride, carbide, oxide, sulfide, and *etc*. were reported. The AEAPS spectra of the $3d_{5/2}$ and $3d_{3/2}$ levels of La in the elemental state and LaH_3 were presented.[135] Since no high binding energy satellites were observed in the $3d_{5/2}$ and $3d_{3/2}$ levels for LaH_3, the lowest energy peak was assigned as the transition of the 3d electron to the 4f level pulled down below the hydrogen induced band.

The AEAPS and SXAPS spectra of LaB_6 and CeB_6 were discussed in terms of atomic like 4f states.[136] It was found that the fine structure reflects multiplet structures of the excited configuration modified by state-selective excitation probabilities near the threshold and, in SXAPS, by dipole selection rules. SXAPS was applied to the metallic glass $Co_{58}Ni_{10}Fe_5B_{16}Si_{11}$ and a drastic change upon crystallization was shown for the B 1s spectrum.[132]

It was pointed out that the energy separation between the main peak and the shoulder in the AEAPS Ti $2p_{3/2}$ spectrum of TiN corresponds to that of empty states in XAS.[133] AEAPS data of TiN_x films indicated the direction of charge transfer from Ti to N and a decrease in the correlation energy with increasing nitrogen content was observed.[141]

The APS spectra of WC,[119] TiC,[124,126,133] and carbon on Si(100)[7] were presented. Catalytic activities of WC were discussed to compare with electronic structures of Pt. Diffraction effects[124,126] and the contribution of secondary electrons to the AEAPS spectra[126] were investigated for a TiC(100) surface.

Many oxides (Cr_2O_3,[121] TiO_2,[123,133,142] Yb_2O_3,[127] La_2O_3,[127] YVO_4,[128] vanadium oxides,[130] $Ca_2V_2O_7$,[131] $Na_{0.33}V_2O_5$,[134] CeO_2,[136] MnO,[139,140] NiO,[143] and CoO[143]) were studied (also see references for metals, alloys, and chemisorptions).

The features of the Ti $2p_{3/2}$ and O 1s spectra for TiO_2(110) and (001) were found to be similar to those of the corresponding XAS spectra.[142] The result was discussed in terms of the "approximate dipole selection rule".[41] The results on NiO(110) and CoO(100) indicated that the features of the Ni 2p (Fig. 11), Co 2p, and O 1s (Fig. 12) spectra are also similar to those of the corresponding XAS spectra. This result suggested that the "approximate dipole selection rule"[41] could be applied to the excitation.[143]

One- (core electron energy-loss spectroscopy, CEELS) and two (APS)-electron excitation into empty states were investigated and compared for MnO(100).[139,140] The features of the O 1s spectra were found to be very similar in both but those of the Mn 2p were different: two-electron excitation was observed for APS.

The result of the $3d_{5/2}$ and $3d_{3/2}$ lines of Yb_2O_3 indicated that the availability of vacant 4f atomic states to accept both the excited d electron and the incident electron was necessary to obtain a strong peak.[127]

The APS spectra of transition metal dichalcogenides (TiS_2,[120,122,125] $TiSe_2$,[120,122] VS_2,[129] VSe_2,[120,122,129] ZrS_2,[122] and $ZrSe_2$,[122]) were presented. The results indicated that the spectra are in good agreement with the predictions of a conduction band self-convolution model. The doublet peaks were shown to be due to the crystal field splitting of d-orbitals in octahedrally co-ordinated transition metal dichalcogenides.

8 Chemisorptions and Reactions[144-157]

The first chemisorption study by APS was carried out on Cr with oxygen.[144] The O 1s threshold was observed at 529.1 eV and the Cr $2p_{3/2}$ threshold energy was increased from 573.5 to 574.1 eV upon adsorption.

The oxidation[146] and chemisorption of N, C, and S[145,147,149] on transition metals were extensively studied by SXAPS using a silicon diode detector.[17] The O 1s spectra exhibited single- and multi-peak at the threshold in the chemisorption regime and oxides, respectively (Fig. 13). The O 1s, Ca 2p, Sr $2p_{3/2}$, and Ba $3d_{5/2}$ spectra for evaporated films of Ca, Sr, and Ba reacted with oxygen were measured.[148] The result showed similar results on the transition metals.

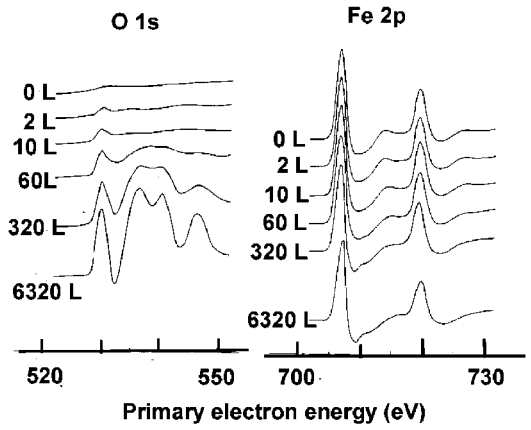

Fig. 13 APS O 1s and Fe 2p spectra for different oxygen exposures (1 L = 1×10^{-6} Torr s) to a Fe metal at RT.[146]

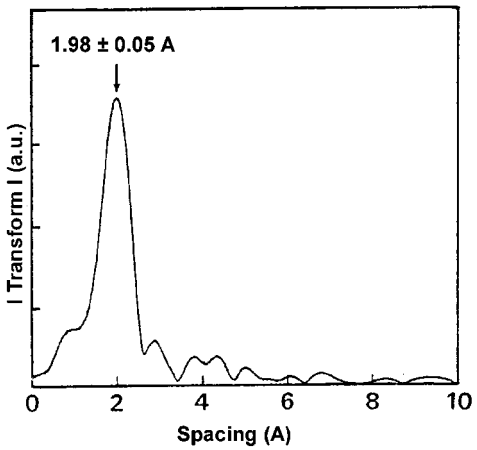

Fig. 14 Fourier transform of the extended fine structures of the APS O 1s spectrum for oxygen on Al(100).[169] The peak at 1.98 ± 0.05 Å was obtained as the O–Al spacing, suggesting that the oxygen lies under the top layer of Al.

The 1s spectra of C, N, and O chemisorbed on Cr, Mo, and W were also presented and the features of them were similar to the above results.[150] The threshold energies for the carbided, nitrided, and oxidized surfaces are listed in the reference.

The chemisorption of oxygen on Ti(0001) was investigated using AEAPS and DAPS.[151] A strong band of states just above the Fermi level was found to be localized near the surface. This band of surface states broadened with increasing temperature and was suppressed by exposure to oxygen.

The self-deconvoluted spectrum of Ni $2p_{3/2}$ for oxidized Ni was found to be consistent with theoretical models of localized and itinerant states.[152] The reaction of thin films of Ti with a Si substrate and Ba-activated oxidation on Ni were studied by AEAPS and DAPS.[154,155] Changes in the APS spectra for an oxidation process of La, Ce, Cr, and Ti were also reported.[156]

The DAPS spectra of a Pt(100) –1 × 1 surface were measured and the spectral features were found to be in good agreement with those of calculated electronic structures.[157] A comparison of experimental and theoretical data showed that hydrogen atoms interact with Pt atoms in the second layer.

9 Depositions[158-164]

The DAPS Ti 2p spectra of Ti thin films deposited on Cu(111) were reported.[158] The result of the growth of Ti on Cu(111) indicated that Cu atoms donate electrons to Ti in TiCu and $TiCu_3$ alloys, leading to the appearance of d-band holes on the Cu sites.

The initial growth of Ti on Si(111) and (100) was studied by DAPS and the result showed the development of a structure characteristic of a pure Ti surface, beginning at coverage of less than a monolayer.[159] The DAPS results were inconsistent with the intermixing of Ti and Si on either Si(111) or (100) at room temperature. Measurements of the AEAPS spectra of $TiSi_2$ thin films prepared by evaporative deposition of Ti on Si(111) were performed.[160] The Ti $2p_{3/2}$ spectra showed a positive shift of about 3 eV. This peak exhibited a broadening compared to that of elemental Ti, indicating bonding between Ti and Si in $TiSi_2$.

The strength of the AES and AEAPS $2p_{3/2}$ and 2s signals of Cr and Ti was measured as a function of the Cr overlayer on a Ti substrate.[161] No significant differences between the information depth of both methods were found. The APS $2p_{3/2}$, $2p_{1/2}$, and 2s spectra of Ti, Cr, Mn, and Ni were measured as a function of their film thickness and APS signal formation was discussed.[162,163]

The spectra of Ti and Ni thin films were measured as a function of the thickness and the elastic contribution of Auger electrons to the AEAPS signal was studied both experimentally and theoretically.[164] The result suggested that the surface sensitivity of the high-energy APS is higher by a factor of about two compared to AES.

10 Fine Structures[165-174]

Fine structures above APS signals were first observed for Cr and oxidized Cr,[144] where it was shown that there were different structures in different surfaces. The fine structure variations above the thresholds for excitation of the V 2p and 2s states were studied in detail.[165,167] The structures were found to extend for several hundred electron volts. The structure exhibited periodicities in k (k-space) and was suggested to result from interference of an outgoing spherical wave of a scattered electron with backscattered components from neighboring atoms. It was pointed out that the structure appeared to be analogous to extended x-ray adsorption fine structure (EXAFS). However, attempts to extract interatomic spacings by Fourier inversion had problems on multiple scattering effects and other complications.

A general formalism was presented for calculation of the fine structures in SXAPS and AEAPS spectra.[166] Electronic wave functions similar to those used in LEED theories were employed to describe the incident electron and the excited final state electron. The problem of calculating the excitation matrix element was discussed. Model calculations were performed for clusters of Ni atoms and oxygen on Ni(100). It was pointed out that multiple-scattering effects were important in the analysis of experimental data. The model calculation showed that the multiple scattering effects introduce an overall phase shift into the calculated curves. The result indicated that it might be feasible to simply extract at least the nearest-neighbor spacing from the APS extended fine structures.[168]

An EAPFS (extended appearance potential fine structure) of oxygen adsorbed on Al(100) was measured and the O–Al spacing was determined to be 1.98 ± 0.05 Å (Fig. 14), suggesting that oxygen lies under the top layer.[169] The EAPFS

were also measured for the As stabilized GaAs(001) surface and the Ga–As and As–As distances at the surface were determined.[173] The result was consistent with the surface structure proposed from results measured by LEED and photoemission. EAPFS and SEELFS (surface extended energy-loss fine structure) were measured on Ti deposited on Si(111).[174] The Ti 2p edge extended fine structure was found to satisfy the dipole pseudo-selection-rule ($\Delta\ell = +1$). Measurements at 400°C data (TiSi) found that the Ti-Si bond spacing was 2.39 ± 0.4 Å, which is in agreement with the predicted value of 2.37 Å.

11 References

1. G. Shinoda, T. Suzuki, and S. Kato, *Phys. Rev*., **1954**, *95*, 840.
2. R. L. Park, J. E. Houston, and D. G. Schreiner, *Rev. Sci. Instrum*., **1970**, *41*, 1810.
3. R. L. Park and J. E. Houston, *J. Vac. Sci. Technol*., **1973**, *10*, 176.
4. R. L. Park and J. E. Houston, *J. Vac. Sci. Technol*., **1974**, *11*, 1.
5. G. Ertl and J. Küppers, "*Low Energy Electrons and Surface Chemistry*", **1974**, Chap. 5, Verlag Chemie, Weinheim, Germany.
6. R. L. Park, *Surf. Sci*., **1975**, **48**, 80.
7. R. L. Park and Y. Fukuda, "*Charaterization of Metal and Polymer Surfaces I*", ed. L. H. Lee, **1977**, Academic Press, 105 - 125.
8. R. L. Park, *Science*, **1988**, *241*, 1839.
9. L. Eckertová, *Surf. Sci*., **1988**, *200*, 490.
10. W. B. Nottingham, *Phys. Rev*., **1935**, *47*, 806.
11. W. L. Baun, M. B. Chamberlain, and J. S. Solomon, *Rev. Sci. Instrum*., **1973**, *44*, 1421.
12. M. B. Chamberlain and W. L. Baun, *Rev. Sci. Instrum*., **1974**, *45*, 545.
13. S. Andersson, H. Hammarqvist, and C. Neyberg, *Rev. Sci. Instrum*., **1974**, *45*, 877.
14. R. S. Withers and R. N. Lee, *Rev. Sci. Instrum*., **1979**, *50*, 326.
15. J. Kirschner, *Solid State Commun*., **1984**, *49*, 39.
16. G. Rangelov, K. Ertl, F. Passek, M. Vonbank, S. Bassen, J. Reimuth, M. Donath, and V. Dose, *J. Vac. Sci. Technol., A*, **1998**, *16*, 2738.
17. R. L. Gerlach, J. E. Houston, and R. L. Park, *Appl. Phys. Lett*., **1970**, *16*, 179.
18. R. L. Gerlach, *Surf. Sci*., **1971**, *28*, 648.
19. J. Kirschner and P. Staib, *Phys. Lett. A*, **1973**, *42*, 335.
20. J. Kirschner and P. Staib, *Appl. Phys. B*, **1975**, *6*, 99.
21. R. L. Park and J. E. Houston, *Surf. Sci*., **1971**, *26*, 664.
22. R. G. Musket and S. W. Taatjes, *J. Vac. Sci. Technol*., **1972**, *9*, 1041.
23. A. Kluge, *Rev. Sci. Instrum*., **1975**, *46*, 1179.
24. R. L. Long and L. C. Beavis, *Rev. Sci. Instrum*., **1972**, *43*, 939.
25. R. L. Lee, *Rev. Sci. Instrum*., **1977**, *48*, 1603.
26. W. L. Baun, M. B. Chamberlain, J. S. Solomon, *Rev. Sci. Instrum*., **1973**, *44*, 1419.
27. L. Papagno and R. Scarmozzino, *Thin Solid Films*, **1980**, *70*, 249.
28. J. E. Houston, *Rev. Sci. Instrum*., **1974**, *45*, 897.
29. L. Eckertová and J. Pavluch, *Czech. J. Phys*., **1984**, *34*, 622.
30. U. Kolac, M. Donath, K. Ertl, H. Liebl, and V. Dose, *Rev. Sci. Instrum*., **1988**, *59*, 1933.
31. B. D. Padalia, P. S. Shinde, A. V. Korgaonkar, and W. C. J. Carvalho, *Rev. Sci. Instrum*., **1991**, *62*, 1109.
32. P. S. Shinde and B. D. Padalia, *Nucl. Instrum. Methods Phys. Res., Sect. B*, **1993**, *82*, 196.
33. G. E. Laramore, *Phys. Rev. Lett*., **1971**, *27*, 1050.
34. G. E. Laramore, *Solid State Commun*., **1972**, *10*, 85.
35. S. Lundqvist and G. Wendin, *J. Electron Spectrosc. Relat. Phenom*., **1974**, *5*, 513.
36. G. Wendin and K. Nuroh, *Phys. Rev. Lett*., **1977**, *39*, 48.
37. K. Nuroh and G. Weiden, *Phys. Rev. B*, **1981**, *24*, 5533.
38. R. Patrick, S. M. Bose, and P. Longe, *Phys. Rev. B*, **1985**, *32*, 3507.
39. R. Patrick, S. M. Bose, and P. Longe, *Phys. Rev. B*, **1985**, *32*, 6286.
40. R. S. Patrick, S. M. Bose, and P. Longe, *Phys. Rev. B*, **1986**, *34*, 5900.
41. M. J. Mehl and T. L. Einstein, *Phys. Rev. B*, **1987**, *36*, 9011.
42. J. del Barco and J. Ferron, *Surf. Sci*., **1990**, *232*, 393.
43. J. Ferron, J. L. del Barco, and E. C. Goldberg, *Surf. Sci*., **1990**, *240*, L579.
44. W. Nolting, G. Geipel, and K. Ertl, *Phys. Rev. B*, **1991**, *44*, 12197.
45. W. Nolting, G. Geipel, and K. Ertl, *Phys. Rev. B*, **1992**, *45*, 5790.
46. M. Potthoff, J. Braun, G. Borstel, and W. Nolting, *Phys. Rev. B*, **1993**, *47*, 12480.
47. P. Valášek, W. von der Linden, and V. Dose, *Phys. Rev. B*, **1995**, *51*, 7471.
48. H. Ebert and V. Popescu, *Phys. Rev. B*, **1997**, *56*, 12884.
49. J. E. Houston and R. L. Park, *Phys. Rev. B*, **1972**, *5*, 3808.
50. R. L. Park and J. E. Houston, *Phys. Rev. B*, **1972**, *6*, 1073.
51. S. Yamamoto, *J. Appl. Phys*., **1973**, *12*, 463.
52. C. Webb and P. M. Wlliams, *Phys. Rev. Lett*., **1974**, *33*, 824.
53. G. Ertl and K. Wandelt, *Surf. Sci*., **1975**, *50*, 479.
54. J. T. Grant, M. P. Hooker, and T. W. Haas, *Surf. Sci*., **1975**, *51*, 433.
55. Y. Fukuda, W. T. Elam, and R. L. Park, *Phys. Rev. B*, **1977**, *16*, 3322.
56. S. Kato, R. Konishi, and S. Mogami, *J. Jpn. Appl. Phys*., **1979**, *18*, 835.
57. V. Dose and G. Reusing, *J. Electron Spectrosc. Relat. Phenom*., **1982**, *27*, 261.
58. S. W. Schultz, K.-Th. Schleicher, D. M. Dück, and H.-U. Chun, *J. Vac. Sci. Technol., A*, **1984**, *2*, 822.
59. D. Chopra, H. W. Axe, and T. K. Hatwar, *J. Electron Spectrosc. Relat. Phenom*., **1984**, *33*, 141.
60. J. Pavluch and L. Eckertová, *Surf. Sci*., **1985**, *162*, 896.
61. V. Dose, R. Drube, and A. Härtl, *Solid State Commun*., **1986**, *57*, 273.
62. V. Donchev, K. Kanev, and C. Tenchov, *Vacuum*, **1986**, *36*, 655.
63. D. M. Pease, *Phys. Rev. B*, **1992**, *46*, 8790.
64. C. J. Powell, N. E. Erickson, and D. E. Ramaker, *Phys. Scrip*., **1992**, *T41*, 175.
65. E. Batkilin, S. Dorfman, and J. Felsteiner, *Phys. Lett. A*, **1994**, *192*, 273.
66. J. Slezák and J. Pavluch, *J. Electron Spectrosc. Relat. Phenom*., **1997**, *83*, 255.
67. J. A. Bearden and A. F. Burr, "*Atomic Energy Levels*", **1965**, U. S. Atomic Energy Commission, NYO 2543-1, Oak Ridge, Tenn.
68. M. B. Chamberlain and W. L. Baum, *J. Vac. Sci. Technol*., **1974**, *11*, 441.
69. M. S. Murthy and P. A. Readhead, *J. Vac. Sci. Technol*., **1974**, *11*, 837.

70. W. E. Harte, P. S. Szczepanek, and A. J. Leyendecker, *Phys. Rev. Lett*., **1974**, *33*, 86.
71. G. Wendin and K. Nuroh, *Phys. Rev. Lett*., **1977**, *39*, 48.
72. G. Crecelius, G. K. Werthheim, and D. N. E. Bubuchanan, *Phys. Rev. B*, **1978**, *18*, 6519.
73. W. Jaschinski and S. Methfessel, *J. Magn. Magn. Mater*., **1979**, *13*, 161.
74. J. Kanski and P. O. Nilsson, *Phys. Rev. Lett*., **1979**, *43*, 1185.
75. Z. Y. Hua, J. Zhuge, C. S. Fan, H. X. Chen, X. L. Pan, and J. L. Huang, *J. Vac. Sci. Technol*., **1980**, *17*, 211.
76. D. Chopra, G. Martin, H. Naraghi, and L. Martinez, *J. Vac. Sci. Technol*., **1981**, *18*, 44.
77. W. E. Harte, P. S. Szczepanek, and A. J. Leyendecker, *J. Less Comm. Metals*, **1983**, *93*, 189.
78. T. K. Hatwar and D. R. Chopra, *J. Electron Spectrosc. Relat. Phenom*., **1985**, *36*, 319.
79. T. K. Hatwar and D. R. Chopra, *Appl. Surf. Sci*., **1985**, *22 – 23*, 267.
80. D. R. Chopra, A. R. Chourasia, and P. V. Prasad, *J. Electron Spectrosc. Relat. Phenom*., **1986**, *41*, 167.
81. D. R. Chopra, *J. Less Comm. Metals*, **1987**, *127*, 373.
82. G. E. Laramore, *Solid State Commun*., **1972**, *10*, 85.
83. J. E. Houston and R. L. Park, *Solid State Commun*., **1972**, *10*, 91.
84. P. O. Nilsson and J. Kanski, *Surf. Sci*., **1973**, *37*, 700.
85. R. L. Park, J. E. Houston, and G. E. Laramore, *Jpn. J. Appl. Phys*., **1974**, *2(Suppl)*., Part 2, 757.
86. J. E. Houston, *Solid State Commun*., **1975**, *17*, 1165.
87. J. Verhoeven and J. Kistemaker, *Surf. Sci*., **1975**, *50*, 388.
88. S. Andersson and C. Nyberg, *Solid State Commun*., **1978**, *28*, 803.
89. R. Konishi, M. Kinoshita, and S. Kato, *Jpn. J. Appl. Phys*., **1982**, *21*, 204.
90. H. J. W. M. Hoekstra, J. C. Fuggle, W. Speier, and D. D. Sarma, *J. Electron Spectrosc. Relat. Phenom*., **1987**, *42*, 27.
91. G. Rangelov and V. Dose, *Surf. Sci*., **1998**, *395*, 1.
92. R. G. Musket, *J. Vac. Sci. Technol*., **1972**, *9*, 603.
93. R. L. Park, J. E. Houston, and D. G. Scheiner, *J. Vac. Sci. Technol*., **1972**, *9*, 1023.
94. K. Wandelt and G. Ertl, *Surf. Sci*., **1976**, *55*, 403.
95. J. T. Grant and M. P. Hooker, *Appl. Surf. Sci*., **1979**, *2*, 433.
96. G. Sicking and B. Jungblut, *Surf. Sci*., **1983**, *127*, 255.
97. T. K. Hatwar and D. Chopra, *Surf. Interface Anal*., **1985**, *7*, 93.
98. V. Dose, G. Reusing, and H. J. Güntherodt, *Solid State Commun*., **1984**, *49*, 1081.
99. D. R. Chopra and T. K. Hatwar, *Surf. Sci*., **1984**, *140*, 216.
100. A. R. Chourasia and D. R. Chopra, *Surf. Sci*., **1988**, *206*, 484.
101. A. R. Chourasia and D. R. Chopra, *Nucl. Instrum. Methods Phys. Res., Sect. B*, **1989**, *40 – 41*, 376.
102. A. R. Chourasia and D. R. Chopra, *J. Less Comm. Metals*, **1989**, *148*, 413.
103. A. R. Chourasia, D. R. Chopra, and S. K. Malik, *J. Vac. Sci. Technol., A*, **1989**, *7*, 2075.
104. P. Valášek, W. von drl Linden, and V. Dose, *J. Electron Spectrosc. Relat. Phenom*., **1995**, *72*, 229.
105. A. R. Chourasia, M. A. Seabolt, R. L. Justiss, D. R. Chopra, and G. Wiesinger, *J. Alloys Compd*., **1995**, *224*, 287.
106. K. Wandelt, G. Ertl, H. C. Siegmann, and P. S. Bagus, *Solid State Commun*., **1977**, *22*, 59.
107. J. Kirschner, *Solid State Commun*., **1984**, *49*, 39.
108. E. M. Haines, R. Clauberg, E. Tamura, and R. Feder, *Solid State Commun*., **1986**, *57*, 669.
109. K. Ertl, M. Vonbank, V. Dose, and J. Noffke, *Solid State Commun*., **1993**, *88*, 557.
110. Th. Detze, M. Vonbank, M. Donath, and V. Dose, *J. Magn. Magn. Mater*., **1995**, *147*, L1.
111. Th. Detze, M. Vonbank, M. Donath, N. Memmel, and V. Dose, *J. Magn. Magn. Mater*., **1996**, *152*, 287.
112. J. Reinmuth, F. Passek, V. N. Petrov, M. Doneth, V. Popescu, and H. Ebert, *Phys. Rev. B*, **1997**, *56*, 12893.
113. G. Rangelov, H. D. Kang, J. Reinmuth, and M. Donath, *Phys. Rev. B*, **2000**, *61*, 549.
114. V. Popescu, H. Ebert, L. Szunyogh, P. Weinberger, and M. Donath, *Phys. Rev. B*, **2000**, *61*, 15241.
115. H. D. Kang, G. Rangelov, J. Reinmuth, and M. Donath, *Surf. Sci*., **2000**, *454 – 456*, 865.
116. J. Fujii, Y. Suzuki, T. Sakai, K. Kuroda, and T. Mizoguchi, *J. Electron Spectrosc. Relat. Phenom*., **2001**, *114 – 116*, 879.
117. H. Kolev, G. Rangelov, J. Braun, and M. Donath, *Phys. Rev. B*, **2005**, *72*, 104415.
118. Ch. Eickhoff, H. Kolev, M. Donath, G. Rangelov, and L. F. Chi, *Phys. Rev. B*, **2007**, *76*, 205440.
119. J. E. Houston, G. E. Laramore, and R. L. Park, *Science*, **1974**, *185*, 258.
120. C. Webb and P. M. Williams, *Phys. Rev. B*, **1975**, *11*, 2082.
121. R. Konishi and S. Kato, *Jpn. J. Appl. Phys*., **1975**, *14*, 1467.
122. C. Webb and P. M. Williams, *Surf. Sci*., **1975**, *53*, 110.
123. R. Konishi and S. Kato, *Jpn. J. Appl. Phys*., **1976**, *15*, 1237.
124. R. L. Park, M. L. den Boer, and Y. Fukuda, Proceedings of the 6th Czechoslovac Conf. Electr. Vac Phys., **1976**, *4*, 53.
125. C. Webb, *Vacuum*, **1977**, *27*, 537.
126. M. L. den Boer, P. I. Cohen, and R. L. Park, *J. Vac. Sci. Technol*., **1978**, *15*, 502.
127. W. E. Harte and P. S. Szcezepanek, *Phys. Rev. Lett*., **1979**, *42*, 1172.
128. I. M. Curelaru and P. O. Nilsson, *J. Phys. Chem. Solids*, **1979**, *40*, 887.
129. H. W. Myron, *Physica B+C*, **1980**, *99*, 243.
130. I. M. Curelaru, *Solid State Commun*., **1980**, *34*, 729.
131. I. M. Curelaru, K.-G. Strid, E. Souninen, E. Minni, and T. Önnhult, *Phys. Rev. B*, **1981**, *23*, 3700.
132. V. Dose and A. Haertl, *Phys. Rev. Lett*., **1981**, *47*, 132.
133. R. Konishi and S. Kato, *Jpn. J. Appl. Phys*., **1984**, *23*, 975.
134. I. M. Curelaru, K.-S. Din, E. Souninen, and E. Minni, *Solid State Ionics*, **1986**, *18 – 19*, 245.
135. A. R. Chourasia and D. R. Chopra, *J. Electron Spectrosc. Relat. Phenom*., **1987**, *43*, 233.
136. H. Hinkers, R. Stiller, and H. Merz, *Phys. Rev. B*, **1989**, *40*, 10594.
137. A. Scheipers and H. Merz, *Int. J. Mod. Phys. B*, **1993**, *7*, 337.
138. A. R. Chourasia, D. R. Chopra, and G. Wiesinger, *J. Electron Spectrosc. Relat. Phenom*., **1994**, *70*, 23.
139. Ch. Henig, C. Untiet, and H. Merz, *J. Electr. Spectr. Relat. Phen*., **1995**, *76*, 547.
140. Ch. Henig and H. Merz, *J. Electron Spectrosc. Relat. Phenom*., **1998**, *93*, 189.
141. A. R. Chourasia and S. J. Hood, *Surf. Interface Anal*., **2001**, *31*, 291.
142. Y. Fukuda, T. Kuroda, and N. Sanada, *Surf. Sci*., **2007**, *601*, 5320.
143. Y. Fukuda, S. Mochizuki, and N. Sanada, *J. Appl. Phys*., **2009**, *106*, 23701.
144. J. E. Houston and R. L. Park, *J. Chem. Phys*., **1971**, *55*, 4601.
145. S. Andersson and C. Nyberg, *Solid State Commun*., **1974**,

15, 1145.
146. C. Nyberg, *Surf. Sci*., **1975**, *52*, 1.
147. S. Andersson and C. Nyberg, *Surf. Sci*., **1975**, *52*, 489.
148. C. Nyberg, *Surf. Sci*., **1977**, *65*, 389.
149. Y. Fukuda, W. T. Elam, and R. L. Park, *Appl. Surf. Sci*., **1978**, *1*, 278.
150. C. Nyberg, *Surf. Sci*., **1979**, *82*, 165.
151. B. T. Jonker, J. F. Morar, and R. L. Park, *Phys. Rev. B*, **1981**, *24*, 2951.
152. H. Scheidt, M. Glöbl, and V. Dose, *Surf. Sci*., **1981**, *112*, 97.
153. R. Konishi, H. Sasaki, and S. Kato, *Jpn. J. Appl. Phys*., **1983**, *22*, 1659.
154. Y. U. Idzerda, E. D. Williams, R. L. Park, and J. Vähäkangas, *Surf. Sci. Lett*., **1986**, *177*, L1028.
155. R. D. Gomez and E. D. Williams, *Surf. Sci*., **1988**, *206*, 289.
156. M. Lu, Q. -J. Zhang, and Z. Hua, *Surf. Sci*., **1995**, *341*, 182.
157. A. R. Cholach and V. M. Tapilin, *J. Mol. Catal. A*, **2000**, *158*, 181.
158. J. Vähäkangas, E. D. Williams, and R. L. Park, *Phys. Rev. B*, **1986**, *33*, 2281.
159. J. Vähäkangas, Y. U. Idzerda, E. D. Williams, and R. L. Park, *Phys. Rev. B*, **1986**, *33*, 8716.
160. D. R. Chopra, A. R. Chourasia, T. R. Dillingham, and K. L. Peterson, *J. Vac. Sci. Technol., A*, **1987**, *5*, 1984.
161. L. Eckertová, T. Jeniček, and J. Pavluch, *Surf. Sci*., **1988**, *200*, 514.
162. J. Pavluch, J. Slezák, and D. Brechlerová, *Vacuum*, **1995**, *46*, 599.
163. J. Pavluch, J. Slezák, and D. Brechlerová, *Vacuum*, **1997**, *48*, 383.
164. I. S. Tilinin, J. Slezák, and J. Pavluch, *J. Electron Spectrosc. Relat. Phenom*., **1997**, *85*, 135.
165. P. I. Cohen, T. L. Einstein, W. T. Elam, Y. Fukuda, and R. L. Park, *Appl. Surf. Sci*., **1978**, *1*, 538.
166. G. E. Laramore, *Phys. Rev. B*, **1978**, *18*, 5254.
167. R. L. Park, P. I. Cohen, T. L. Einstein, and W. T. Elam, *J. Cryst. Growth*, **1978**, *45*, 435.
168. G. E. Laramore, *Surf. Sci*., **1979**, *81*, 43.
169. M. L. den Boer, T. L. Einstein, W. T. Elam, R. L. Park, L. D. Roelofs, and G. E. Laramore, *Phys. Rev. Lett*., **1980**, *44*, 496.
170. G. E. Laramore, T. L. Einstein, L. D. Roelofs, and R. L. Park, *Phys. Rev. B*, **1980**, *21*, 2108.
171. T. L. Einstein, M. L. den Boer, J. F. Morar, and R. L. Park, *J. Vac. Sci. Technol*., **1981**, *18*, 490.
172. M. J. Mehl, T. L. Einstein, and G. W. Bryant, *J. Vac. Sci. Technol. A*, **1984**, *2*, 862.
173. H. Terauchi, S. Sekimoto, N. Sano, H. Kato, and M. Nakayama, *Appl. Phys. Lett*., **1985**, *46*, 148.
174. I. U. Idzerda, E. D. Williams, T. L. Einstein, and R. L. Park, *Phys. Rev. B*, **1987**, *36*, 5941.